

## Initial stages in the epitaxial growth of NaCl on Ge(001)

C.A. Lucas, G.C.L. Wong<sup>1</sup>

*Center for Advanced Materials, Materials Sciences Division, Lawrence Berkeley Laboratory, University of California, Berkeley, CA 94720, USA*

C.S. Dower

*Department of Physics, University of Edinburgh, Edinburgh EH9 3JZ, UK*

F.J. Lamelas and P.H. Fuoss

*AT&T Bell Laboratories, 600 Mountain Avenue, Murray Hill, NJ 07974, USA*

Received 3 September 1992; accepted for publication 16 December 1992

We have performed an in situ X-ray scattering study of the initial stages of NaCl/Ge(001) heteroepitaxy. The  $c(4 \times 2)$  surface reconstruction, characteristic of Ge(001) at low temperature, is suppressed immediately upon deposition of NaCl. However, the  $(2 \times 1)$  symmetry of the surface unit cell is preserved, even after 6 monolayers (ML) of NaCl have been grown. Analysis of the in-plane, half-integer Bragg reflections, specific to the surface reconstruction, supports a model in which the Ge dimer remains and sodium is adsorbed in the “valley” site. Subsequent growth of NaCl on the modified surface occurs through the formation of islands with the thickness of a triple layer (3 ML), which fill in until the triple layer is complete.

### 1. Introduction

The microscopic mechanisms involved in the initial stages of interface formation between ionic and covalent materials is an area of fundamental interest in solid state physics [1]. However, due to the inaccessibility of buried interfaces to standard surface probes and the problems associated with studying insulating materials because of surface charging and electron beam damage, there is little understanding of the growth of ionic/covalent heterostructures. Perhaps the most widely studied ionic/covalent system is  $\text{CaF}_2/\text{Si}(111)$ , where there has been considerable controversy over the structure of the interface [2–4]. Much of this controversy is generated by the fact that interpretation of many experiments depends

on a detailed understanding of the growth behaviour, e.g. whether classification into one of the known growth modes is applicable [5]. The situation is further complicated when differences in sample preparation cause varying results.

Recently it has been shown that the conditions under which alkali halide single crystals grow from molecular beams are significantly different from those of semiconductors and metals [6]. This is due to the ionic bonding which is weak on terraces and strong at ledges. The cubic NaCl structure, with a lattice constant  $a_0 = 5.63 \text{ \AA}$ , is closely lattice matched to germanium ( $a_0 = 5.66 \text{ \AA}$ ). NaCl/Ge is, therefore, an ideal candidate for studying the mechanisms of ionic/covalent heteroepitaxy. The conditions under which uniform NaCl films can be grown by molecular beam epitaxy (MBE) on Ge(001) have been identified in a low energy electron diffraction (LEED) study [7]. The sharpest LEED patterns, indicative of

<sup>1</sup> Also at: Department of Physics, University of California, Berkeley, USA.

large crystalline domains, were obtained when the sample was cooled to 150 K during growth, although the structure at the interface was unknown. X-ray diffraction is a powerful probe for studying buried interfaces, due to the high penetration of the X-ray beam and the weak interaction of X-rays with matter which enables simple kinematical scattering models to be employed. In this paper we present results of an in situ X-ray scattering study of the early stages of NaCl deposition onto a clean Ge(001) surface. By combining grazing incidence X-ray scattering and X-ray reflectivity measurements we gain insight into the physical mechanisms governing the initial bonding at the interface, and the subsequent overlayer growth.

## 2. Experimental

The experiments were performed on beamline X16A of the National Synchrotron Light Source (NSLS) at Brookhaven National Laboratory, using an ultrahigh vacuum (UHV) chamber coupled to a five circle diffractometer [8]. Measurements were taken on two germanium samples, with surfaces offcut by  $\sim 1.4^\circ$  (sample I) and  $\sim 0.35^\circ$  (sample II) to the (001) lattice planes, as measured by X-ray diffraction prior to the experiment. The miscut in both samples was approximately along the [110] crystallographic direction. After loading into the UHV chamber the sample surface was cleaned by repeated cycles of sputtering and annealing (1/2 h with 800 eV  $\text{Ar}^+$  ions, followed by a 5 minute anneal at  $700^\circ\text{C}$  and cooling at  $\sim 40^\circ/\text{min}$ ). Although a strong LEED pattern, with  $(1 \times 2)$  and  $(2 \times 1)$  superlattice reflections, was observed after two sputter-anneal cycles, the cleaning procedure was repeated until there was no improvement in the widths and intensities of the  $\langle 2 \times 1 \rangle$  peaks measured by X-ray diffraction. This typically took 6–8 cycles. For NaCl deposition the sample was cooled to  $\sim 180$  K by thermal contact with a liquid nitrogen reservoir. The temperature was controlled by resistive heating and measured by a thermocouple in contact with a Ta ring attached to the back of the sample. NaCl (Solon Technologies, Inc.) was

evaporated from a BN crucible at  $630^\circ\text{C}$ , which gave a deposition rate of approximately  $3 \text{ \AA}/\text{min}$ . The base pressure in the UHV chamber was  $4 \times 10^{-11}$  Torr, typically increasing to the mid  $10^{-10}$  Torr range during growth. All measurements were made with a monochromatic X-ray beam ( $\lambda = 1.238 \text{ \AA}$ ), focussed to a  $1.0$  (horizontal)  $\times 1.5 \text{ mm}^2$  (vertical) spot on the sample. The sample was mounted with its surface normal in the horizontal plane and horizontal slits were used to define the resolution along the  $L$  direction, i.e. the surface normal in reciprocal space. Scattered X-rays were detected by a position sensitive detector after passing through a  $50$  (horizontal)  $\times 1 \text{ mm}^2$  (vertical) entrance slit at a distance of  $\sim 500$  mm from the sample. The detector was binned such that the angular resolution was  $\sim 0.35^\circ$  in the horizontal scattering plane (along  $L$ ). The instrumental resolution has been discussed in detail elsewhere [9,10]. All results were normalised to the incident beam intensity by measuring a small fraction of the monochromatic beam scattered into a monitor detector.

## 3. Results and discussion

### 3.1. In-plane X-ray diffraction and rod scans

It is well established that the clean Ge(001) surface exhibits a two-domain  $(2 \times 1)$  reconstruction, which consists of rows of atomic dimers created through the pairing of nearest-neighbour surface atoms [11]. This gives rise to Bragg reflections at half-integer positions, with intensities that are uniquely related to the structure of the surface unit cell. A set of reflections was measured, in each case by fixing the detector at the appropriate Bragg angle and rotating the sample about the surface normal ( $\theta$  scan) to obtain an integrated intensity. A typical  $\theta$  scan is shown in fig. 1a for the  $(\frac{3}{2}, 0, 0.05)$  Bragg reflection. The reflections are indexed using the standard LEED notation, in which the surface unit cell is related in reciprocal space to the conventional cubic unit cell by  $(1 \ 0 \ 0)_{\text{surf}} = \frac{1}{2}(2 \ \bar{2} \ 0)_{\text{cub}}$ ,  $(0 \ 1 \ 0)_{\text{surf}} = \frac{1}{2}(2 \ 2 \ 0)_{\text{cub}}$  and  $(0 \ 0 \ 1)_{\text{surf}} = (0 \ 0 \ 1)_{\text{cub}}$ . In-plane reflections were measured at  $L = 0.05$ , correspond-

ing to a momentum transfer of  $0.055 \text{ \AA}^{-1}$  out of the surface plane. The incidence and exit angle of the X-ray beam with respect to the sample surface was  $\sim 0.3^\circ$ , slightly above the critical angle for total external reflection.

The solid line in fig. 1a is a fit to the data with a Lorentzian lineshape and a constant background. The background subtracted integrated intensities, obtained from such Lorentzian fits to the data, are proportional to the surface structure factor intensities after correction for the Lorentz factor [9,10]. In both Ge samples the intensity distribution between the two domains was roughly equal. For sample, I, the widths of the  $\langle \frac{3}{2}, 0 \rangle$  reflections gave a domain size of 42 and 183  $\text{\AA}$  respectively along, and perpendicular to, the miscut direction. For sample II the domain sizes were 290 and 500  $\text{\AA}$  (the peak widths were considerably broader than the in-plane instrumental resolution which, from measurement of bulk Bragg reflections, corresponded to a coherence length of  $\sim 8000 \text{ \AA}$ ). As the miscut was approximately along the  $[10]_{\text{surf}}$  direction, the domain sizes indicate that in both samples the steps on the surface were primarily of monolayer height.

Since good agreement was found between the two samples we focus on the structure factors obtained from sample II and these are shown in table 1. Using the two layer model of the surface unit cell, depicted in fig. 1b, we follow the work of Grey et al. [12] and apply a least-squares fitting routine to the data with four parameters: bond length of the symmetric dimer, second layer relaxation along the dimer bond, an isotropic Debye–Waller factor and an overall scale factor (the structural parameters are indicated in fig. 1b). The structure factor for a particular reflection ( $hk$ ) is given by [9]

$$F_{hk} = \sum_j f_j(Q) \exp[2\pi i(hx_j + ky_j)],$$

where the sum extends over all the atoms at atomic positions  $(x_j, y_j)$  in the unit cell,  $Q$  is the in-plane momentum transfer, and  $f_j$  is the atomic scattering factor which includes the Debye–Waller factor  $\exp[-B_j Q^2/16\pi^2]$ . For bulk Ge  $B = 0.58 \text{ \AA}^2$ . This calculation represents the structure of the unit cell projected onto the surface plane, i.e. with perpendicular momentum transfer  $L = 0$ . The calculated structure factors are shown

Table 1  
Measured structure factor intensities  $|F_{\text{exp}}|^2$  for the clean and NaCl covered Ge( $2 \times 1$ ) surface at room temperature (sample II)

$h$	$k$	Clean Ge Surface			NaCl/Ge				
		$ F_{\text{exp}} ^2$	$\sigma_{\text{exp}}$	$ F_{\text{calc}} ^2$	$ F_{\text{exp}} ^2$	$\sigma_{\text{exp}}$	$ F_{\text{calc}}^{\text{Ge}} ^2$	$ F_{\text{calc}}^{\text{Cl}} ^2$	$ F_{\text{calc}}^{\text{Na}} ^2$
$\frac{1}{2}$	0	10.0	1.9	11.6	5.0	1.4	11.3	3.6	5.6
$\frac{1}{2}$	1	5.2	1.1	6.2	5.0	1.6	4.1	7.4	6.5
$\frac{1}{2}$	2	6.1	1.5	5.9	4.2	1.0	4.7	4.1	4.2
$\frac{1}{2}$	3	2.5	0.4	2.2	2.1	0.6	1.0	1.8	1.9
$\frac{3}{2}$	0	22.4	1.7	20.2	26.6	1.3	20.8	27.0	26.4
$\frac{3}{2}$	1	7.2	6.0	7.3	3.2	0.3	3.8	3.1	3.2
$\frac{3}{2}$	2	12.3	1.2	11.8	15.3	1.9	9.9	13.4	14.7
$\frac{5}{2}$	0	0.07	0.07	0.12	0.8	0.1	1.0	0.8	0.8
$\frac{5}{2}$	1	2.3	0.2	2.4	2.4	0.1	2.5	2.4	2.4
$\frac{7}{2}$	0	1.3	0.4	1.7	0.7	0.5	0.2	0.4	0.3

The NaCl film was grown by 240 s of deposition with the sample held at  $\sim 180 \text{ K}$ . The reflections shown are independent, and the errors result from a combination of reproducibility of symmetry equivalent reflections and counting statistics.  $|F_{\text{calc}}|^2$  are the calculated structure factor intensities using the surface unit cell in fig. 1b. For the NaCl covered surface  $|F_{\text{calc}}^{\text{Ge}}|^2$  uses the same model as for the clean surface, whereas  $|F_{\text{calc}}^{\text{Na}}|^2$  and  $|F_{\text{calc}}^{\text{Cl}}|^2$  are calculated with respectively an additional Na or Cl atom in the surface unit cell. Potential adsorption sites are shown in fig. 1b. In all cases  $\chi^2$  is calculated by  $\chi^2 = [1/(N - P)] \sum_{k=1}^N (F_{\text{exp}}^k - F_{\text{calc}}^k)^2 / \sigma_k^2$ , where  $N$  is the number of structure factors and  $P$  is the number of free parameters. The parameters are listed in table 2.

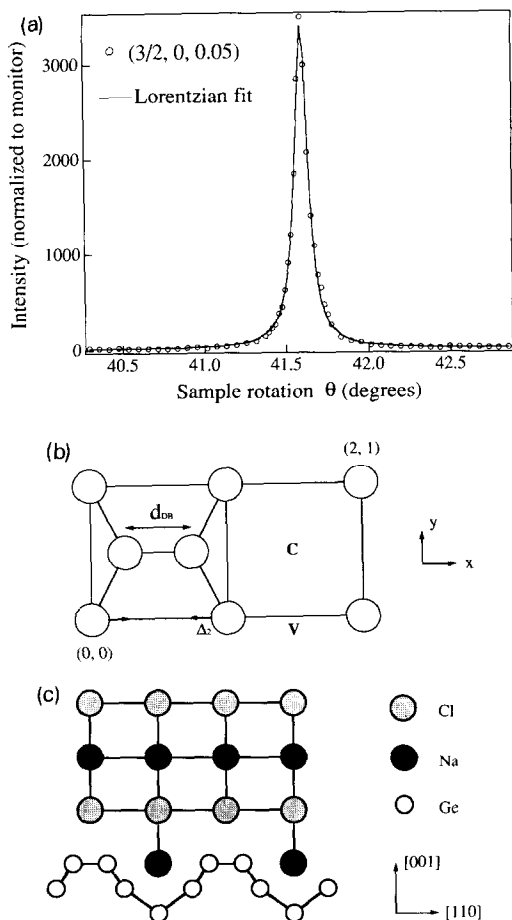


Fig. 1. (a) A  $\theta$  scan through the  $(\frac{3}{2}, 0, 0.05)$  Bragg rod for the clean Ge(001) surface (sample II) at room temperature. The solid line is a fit to the data using a Lorentzian profile and a constant background. (b) Projection of the dimer model of the Ge(001)(2x1) reconstruction onto the surface plane [12]. The arrows show the directions of relaxation. An asymmetric dimer would be represented by an  $x$  shift in the center position of the dimer. Also shown are the “cave” site (C) and “valley” site (V) proposed for alkali metal adsorption on the Si(001) surface [16,17]. (c) A section through the Ge(110) plane showing the location of the adatom and the subsequent NaCl overlayer. The registry of the overlayer was determined by crystal truncation rod measurements.

in table 1 according to the structural parameters in table 2. The results are in good agreement with the previous study [12]. With the limited data set shown it is difficult to extract any information about dimer buckling. Such analysis involves a calculation of the scattering from a random array

of tilted dimers, and, for comparison with experiment, would require a thorough measurement of both the Bragg and diffuse X-ray scattering in reciprocal space.

Fölsch et al. [7] demonstrated that NaCl films grown on Ge(001) exhibited the sharpest LEED patterns when the substrate was cold (150 K) during deposition. We cooled our samples to  $\sim 180$  K prior to growth. This results in an ordering of the surface into a  $c(4 \times 2)$  reconstruction [13,14], and is characterised by extra Bragg reflections at the quarter order positions. Measurements of the  $c(4 \times 2) \rightarrow (2 \times 1)$  phase transition, and a more detailed study of the clean Ge(001) surface will be presented elsewhere [15]. Deposition of NaCl at 180 K caused a systematic change in the in-plane structure factors. In particular, the  $c(4 \times 2)$  reconstruction was completely suppressed, i.e. the peaks at quarter-order positions disappeared, leaving only the  $(2 \times 1)$  superlattice reflections at half-integer positions. Structure factors for the NaCl modified surface, at room temperature, are listed in table 1. The measurements were taken after 240 s of NaCl deposition. Identical behaviour was observed after only 40 s of deposition. The results were reproducible on both samples and over a number of separate deposition experiments.

In order to understand how the Ge(001)(2x1) surface may be altered by NaCl deposition, it is important to combine in-plane structural information with some knowledge of the structural changes in the surface normal direction. Due to the two-dimensional nature of the surface unit cell, the intensity at the half-integer Bragg reflections is extended along the surface normal direction in reciprocal space. It is possible to measure this intensity as a function of perpendicular momentum transfer [9,10]. The results, after correction for polarisation, the Lorentz factor and the variation in the active area on the sample surface [10], are shown in fig. 2a. The  $(\frac{3}{2}, 0, L)$  rod is an average of the symmetry equivalent  $(\frac{3}{2}, 0, L)$  and  $(\frac{3}{2}, 0, L)$  rods. The oscillation in the data indicates that the unit cell involves more than just the top two layers at the surface, used to calculate the in-plane structure factors. The period of the oscillation is  $\sim 0.5$  reciprocal lattice units, corre-

Table 2

Parameters in the calculation of structure factors in table 1, using the model shown in fig. 1b

	$d_{DB}$ (Å)	$B$ (Å <sup>2</sup> )	$\Delta_2$ (Å)	$x_i$	$y_i$	$\chi^2$
$ F_{\text{calc}} ^2$	2.30	1.3	0.084	–	–	1.0
$ F_{\text{calc}}^{\text{Ge}} ^2$	2.33	2.9	0.143	–	–	9.9
$ F_{\text{calc}}^{\text{Cl}} ^2$	2.36	0.6	0.134	1.55	0.08	1.3
$ F_{\text{calc}}^{\text{Na}} ^2$	2.35	0.6	0.136	1.54	0.06	0.5

The values of the overall scale factor are not shown. The directions of relaxation and atomic positions are indicated in fig. 1b. The best fit to the NaCl/Ge interface occurs with Na adsorbed at the “valley” site.

sponding to a unit cell extending four layers into the bulk. This is in agreement with previous measurements [12], in which a model involving atomic eight layers into the bulk was derived, based on analysis of four independent half-integer rod scans.

It is instructive to compare the rod scans in fig. 2a measured before, and after, NaCl deposition. Apart from the shift in intensity there is no change in the  $L$  dependence, i.e. the thickness of the unit cell is unchanged. It should, therefore, be possible to account for the measured changes in the in-plane structure factors using the same model as for the clean surface. Using the model in fig. 1b, but in addition allowing the dimer center to shift, which would correspond to a

buckled dimer, it was not possible to obtain a good fit to the data. The best fit gave  $\chi^2 = 9.9$  (see tables 1 and 2). As the thickness of the unit cell is unchanged (from fig. 2), likely adsorption sites for arriving atoms would be the so called “cave” or “valley” sites in between the surface dimers (the sites are indicated in fig. 1b). Occupation of these sites has been suggested for alkali metal absorption on Si(001) [16,17]. We attempted to fit our data by including a Na or Cl atom in the unit cell and varying its atomic coordinates. A Cl atom gives  $\chi^2 = 1.3$  and the calculated structure factors shown in table 1 (the parameters are shown in table 2). However, including a Na atom reduces  $\chi^2$  to 0.5. Including an equal mixture of Na and Cl in the adsorption site,

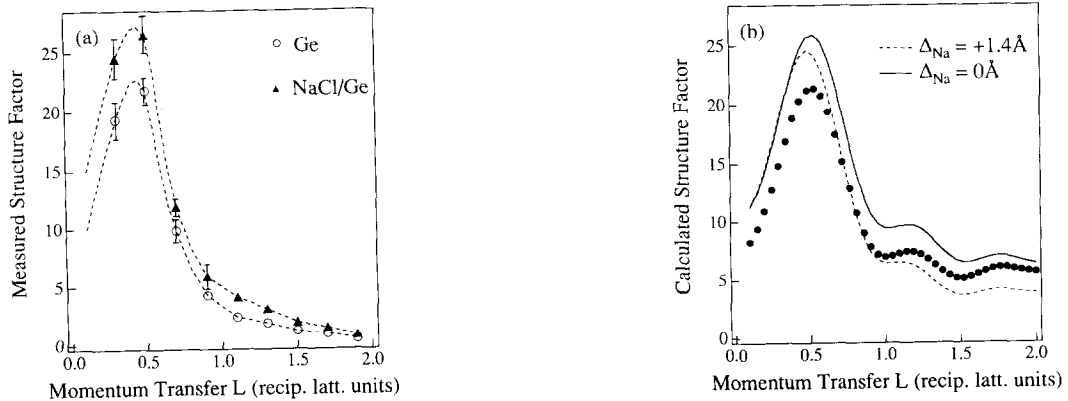


Fig. 2. (a) The  $(\frac{3}{2}, 0, L)$  structure factor intensity as a function of wave vector transfer,  $L$ , perpendicular to the sample surface, for the clean and NaCl covered  $\text{Ge}(2 \times 1)$  surface (sample II). The dashed lines are a guide to the eye. (b) Calculations of the  $(\frac{3}{2}, 0, L)$  scattering according to the model of Grey et al. [12] for the clean surface (filled circles), and adapted to include an extra Na atom, for two different vertical displacements of the atom relative to the Ge dimer, i.e. 0 Å (solid line) and +1.4 Å (dashed line).

as would be the case if NaCl molecules were adsorbed, gave  $\chi^2 = 1.1$ . However, when the NaCl ratio was allowed to vary, the best fit was obtained with only Na being adsorbed. The atomic coordinates (table 2) indicate that the adatom sits at the “valley” site. Although  $\chi^2 < 1$  suggests that no further information can be obtained from the data, the determination of  $\chi^2$  does depend on the accuracy of error calculation, and the errors may be overestimated in our analysis. It is known that Na adsorbed on Si(001) can reside in the “valley” site [16,17]. A combined photoemission/LEED study of halogen covered germanium concluded that Cl was adsorbed on top of the dimer at the Ge(001) surface, thus saturating the remaining broken bonds [18]. This supports our results, which indicate that Na is adsorbed between the Ge dimers. A schematic illustration of the interface structure, as a section through the Ge(110) plane, is shown in fig. 1c. The registry of the NaCl film was confirmed by crystal truncation rod measurements through the (111) bulk Bragg reflection.

An estimate of the height of the adatom above the surface can be obtained by calculation of the  $(\frac{3}{2}, 0, L)$  rod scan using the eight layer model of Grey et al. [12]. Although their model does not exactly fit our data, the same general features are reproduced. We note that the previous measurements were over a reduced  $L$  range ( $L = 0.0-1.0$ ) and in this limit the calculation agrees with our results. There is, however, a clear discrepancy at higher  $L$  values; the calculated scattering is higher than the measured scattering. The decrease in

intensity may be due to surface roughness (such as atomic steps) which is not included in the model calculation. The calculation for the clean surface is shown by the data points in fig. 2b. Addition of the Na atom at the valley site, and at the height of the Ge dimer, causes the observed shift in intensity (solid line). A calculation with the atom displaced upwards (away from the surface) by 1.4 Å is shown by the dashed line (displacing the atom downwards by 1.4 Å gave a similar result). Clearly the solid line gives the best qualitative representation of the changes in the measured scattering, indicating that the Na atom is close to the height of the Ge dimer. An exact determination of the adatom height requires adaptation of the structural model to fit the data, both before and after NaCl deposition. This would only be possible with a much larger data set to allow refinement of the model parameters. The data presented here are insufficient for such analysis.

### 3.2. *Specular X-ray reflectivity*

Specular X-ray reflectivity is a widely used technique which is particularly sensitive to surface layers which differ in electron density from the bulk material [19]. It is therefore ideal for studying growth on a clean surface within a UHV environment [20], as the results can be interpreted unambiguously with a minimum of structural parameters. We measured X-ray reflectivity curves from our samples at various stages of growth by using a small horizontal slit in front of

Table 3  
Parameters used to calculate the reflectivity curves in fig. 3

Curve	Growth time (s)	$\rho_{\text{NaCl}}/\rho_{\text{Ge}}$	$d_{\text{NaCl}}$ (Å)	$\sigma_{\text{NaCl}}$ (Å)	$\sigma_{\text{Ge}}$ (Å)	$(\rho_{\text{NaCl}}/\rho_{\text{Ge}}) \times d_{\text{NaCl}}$
(a)	0	–	–	–	0.7	–
(b)	20	0.02	8.6	0.1	0.9	0.17
(c)	60	0.141	7.9	1.4	0.4	1.11
(d)	120	0.343	8.3	1.9	1.0	2.85
(e)	120	0.187	15.2	0.9	0.4	2.84

The clean Ge surface is fitted by the Fresnel law multiplied by a Debye–Waller factor. The NaCl/Ge data is fitted using a two-layer model (film + substrate) with the parameters: density, film thickness, interface roughness and a scale factor. The formalism used to calculate the reflectivity has been described in detail by Tidswell et al. [21]. For bulk crystals  $\rho_{\text{NaCl}}/\rho_{\text{Ge}} = 0.4$ . The bulk lattice parameter of NaCl is 5.63 Å, corresponding to two monolayers.

the detector, and scanning along the specular rod over the range  $2^\circ$ – $7^\circ$  in incidence angle (this corresponds to a wave vector transfer range of  $0.35$ – $1.24 \text{ \AA}^{-1}$ ). Below  $2^\circ$  the illuminated area was larger than the sample. The upper limit of  $7^\circ$  was determined by the mechanical constraints imposed by the coupling of the diffractometer and UHV chamber. Prior to the measurement rocking scans were performed at the two limits, and in each case these showed a resolution limited peak superimposed on a negligible flat background. Reflectivity curves from sample I at room temperature are shown in fig. 3 (a) for the clean Ge surface, and (b) after 20, (c) 60, and (d) 120 s of NaCl deposition. The data is corrected for polarisation and beam area effects, and normalised to the Fresnel law by multiplying the intensity by  $\theta^4$ . Fits to the data are shown by solid lines and were calculated according to the formalism described explicitly by Tidswell et al. [21]. The parameters to the fits are shown in table 3. For the clean surface a good fit is obtained by multiplying the Fresnel law by a Debye–Waller

type factor  $\exp(-Q^2\sigma^2)$  with  $\sigma_{\text{rms}} = 0.7 \text{ \AA}$ . After NaCl deposition a simple two level model fits the data; the parameters are layer thickness, density, surface roughness, interface roughness and an overall scale factor. This model does not explicitly include the Ge dimer or proposed Na adatom. These features are incorporated into the roughness at the interface.

The most striking result is that the thickness of the layer is constant ( $\sim 8.3 \text{ \AA}$ ) as the deposition time increases. The thickness corresponds to growth as a triple layer of NaCl. Although an islanded structure will give rise to diffuse scattering, there was no appreciable diffuse peak in the transverse scans performed prior to the reflectivity measurements. This could be due to a small island size, which would spread the diffuse scattering over a large angular range and thus appear as a flat background in the region of the specular peak. The surface roughness values in table 3 are fairly constant at the various stages of growth, indicating that the triple-layer islands have smooth surfaces (the presence of a dominant period in the reflectivity curves also supports this model). The thickness is determined by the period of the oscillation in fig. 3 and is unchanged between curves (c) and (d), where the total deposition time has doubled. A further clue to the growth mechanism can be seen in table 3 in the values of  $(\rho d)$ , which is proportional to the amount of material in the triple layer. A discrepancy occurs between (b) 20 and (c) 60 s of growth, as the coverage has not tripled. On the basis of the in-plane structure factor analysis we proposed that initial bonding involved a Na atom incorporated into the Ge surface unit cell. This would not be part of the subsequent triple-layer growth and may account for the majority of NaCl deposition in the first 20 s. If the first 20 s of growth involves formation of this modified interface layer, then growth of the triple-layer has occurred for approximately 0, 40 and 100 s for curves (b), (c), and (d), respectively. The coverage in the triple layer, determined by the reflectivity results, is now in good agreement with the amount of deposited material. The origin of the triple layer growth may be the interfacial strain; a similar behaviour is observed in the growth of Ge on

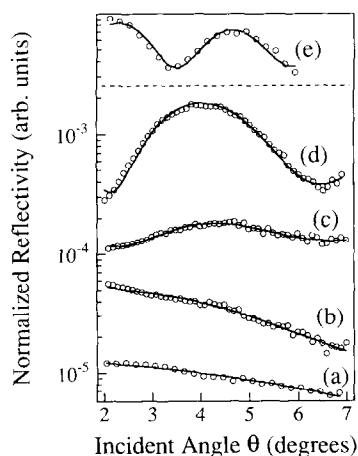


Fig. 3. Reflectivity curves, normalised to the Fresnel reflectivity, for (a) the clean Ge surface (sample I), and after (b) 20 (c) 60 and (d) 120 s of NaCl deposition at a substrate temperature of 180 K. Curve (e) was taken after the sample was heated to 370 K for approximately 5 min. All measurements were performed at room temperature and the data are displaced for clarity. The solid lines are fits to the data according to the parameters in table 3 in a simple two-layer model, i.e. film+substrate. The wave vector transfer  $Q = (4\pi/\lambda) \sin \theta$ , where  $\theta$  is the incidence angle.

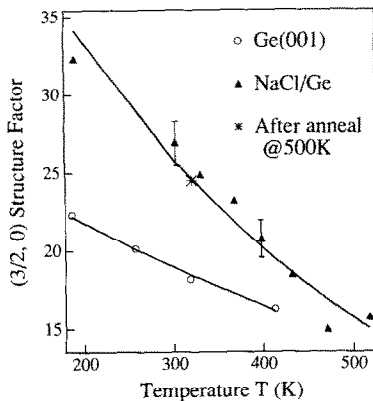


Fig. 4. Temperature dependence of the  $\langle \frac{3}{2}, 0 \rangle$  surface structure factor intensities for the clean and NaCl covered Ge( $2 \times 1$ ) surface (sample I). The NaCl film was prepared by deposition for 120 s with the substrate held at 180 K (the reflectivity is shown in fig. 3(d)). The additional point at 325 K was taken after the sample was cooled following a 5 min anneal at 520 K. The solid lines are calculations using a simple model described in the text.

Si(001), where a metastable 3D phase forms the kinetic pathway for the subsequent macroscopic islanding [22]. Also, epitaxy of NaCl occurs on a Na modified surface, thus presenting a different surface energy problem than that of epitaxy on a clean Ge surface. Formation of a stable triple layer may be the result of a balance between the competing surface energies and the kinetics of the arriving NaCl molecules on the modified surface [6].

### 3.3. Temperature dependence of results

Further insight into the structure and growth mechanisms was obtained by heating the NaCl/Ge samples from the growth temperature (180 K) up to the temperature for NaCl desorption ( $\sim 500$  K). Fig. 4 shows the temperature dependence of the  $\langle \frac{3}{2}, 0 \rangle$  in-plane structure factor for both the clean Ge( $2 \times 1$ ) surface, and the NaCl/Ge( $2 \times 1$ ) interface produced by 120 s of NaCl deposition, i.e. the same film from which the reflectivity curve in fig. was obtained. As in fig. 2, the results are an average of symmetry equivalent reflections. One possible explanation for the observed temperature dependence is that

raising the temperature causes a reduction in surface coverage, either by desorption or islanding, and that the  $\langle \frac{3}{2}, 0 \rangle$  intensity results from the sum of intensities from a clean, and NaCl covered, Ge( $2 \times 1$ ) surface. The reflectivity after annealing to 370 K is shown in fig. 3(e). Clearly the thickness has increased (the fit parameters in table 3 show that it has almost doubled) indicating that the film is islanding. Presumably the triple layer is a metastable state and raising the temperature causes the NaCl to island as determined by the competing surface energies [23]. After heating to 500 K, close to the desorption temperature, the sample was cooled to room temperature and the measurements were repeated. The  $\langle \frac{3}{2}, 0 \rangle$  data point is shown in fig. 4. The reflectivity curve, which is not shown, indicated that the film had roughened severely. However, the intensity of the  $\langle \frac{3}{2}, 0 \rangle$  peak is close to the intensity measured before heating, implying that the Na coverage of the ( $2 \times 1$ ) surface has not significantly changed. The islanding is therefore taking place on top of the modified Ge/Na unit cell. It is interesting to note that Fölsch et al. [7] observed a strong ( $3 \times 1$ ) LEED pattern after desorption of NaCl from a Ge(111) surface. The ( $3 \times 1$ ) superstructure is a characteristic feature of Na absorbed on Ge(111). It is possible that the same mechanism governs the early stages of epitaxy on both Ge(001) and Ge(111) surfaces, i.e. some form of chemisorption in which the NaCl molecule is dissociated.

Assuming that the exponent of the Debye–Waller factor is proportional to the temperature  $T$  [24], it is possible to fit the data in fig. 4 (solid lines) by modifying the atomic form factors in the calculation of the structure factors

$$f'_{\text{Na}} = f_{\text{Na}} \exp(-c_{\text{Na}}T), \quad f'_{\text{Ge}} = f_{\text{Ge}} \exp(-c_{\text{Ge}}T).$$

This also assumes that no significant structural changes occur in the ( $2 \times 1$ ) unit cell as the temperature is changed. For the clean germanium surface  $c_{\text{Ge}} = 0.02$ , whereas for the NaCl covered surface  $c_{\text{Ge}} = 0.032$  and  $c_{\text{Na}} = 0.052$  (the calculation is not very sensitive to the value of  $c_{\text{Na}}$ ). This semi-quantitative analysis indicates that the atoms at the Na/Ge interface can vibrate

more freely than the Ge atoms in the Ge/vacuum-( $2 \times 1$ ) interface. Recently, extremely large anisotropic thermal vibrations of gallium adatoms on a Si(111) surface have been observed in an X-ray standing wave experiment [25]. This effect was attributed to thermal softening of the surface bonding at elevated temperatures. It would be interesting to measure the vibrational modes at the NaCl/Ge interface, for example using electron energy loss spectroscopy (EELS) or X-ray standing wave measurements.

#### 4. Conclusions

We have performed a detailed X-ray scattering study of the early stages of epitaxy of NaCl on a Ge(001)( $2 \times 1$ ) reconstructed surface. Analysis of the non-integer reflections, specific to the surface unit cell, show that the  $(4 \times 2)$  low temperature reconstruction is suppressed upon NaCl deposition but a modified ( $2 \times 1$ ) reconstruction at the interface remains. Comparison of measured and calculated structure factors indicates that the new surface cell contains Na adsorbed at the "valley" site. Presumably the excess Cl is desorbed into the vacuum. NaCl grows on this modified ( $2 \times 1$ ) surface in a triple layer configuration, as evidenced by reflectivity measurements taken by interrupting the growth at various stages during deposition. The formation of these triple-layer islands is particularly interesting, as such a mechanism is not completely described by any of the well known epitaxial growth modes. A similar growth mechanism has been observed in  $\text{CaF}_2/\text{Si}(111)$  epitaxy [5], another example of an ionic/covalent system. Finally, we would like to point out that the NaCl/Ge(001) system would be interesting to study with other surface and interface sensitive experimental techniques. Photoelectron diffraction and photoemission measurements would be able to test our model for epitaxy, and additionally probe the electronic structure at the interface. Such results may give further insight into the issues of bonding, and charge transfer within dimers, at reconstructed semiconductor surfaces.

#### Acknowledgements

We are extremely grateful to Kohei Itoh for providing the Ge substrates, to Peter Eng and Ian Robinson for assistance with beamline X16A, and to the staff and user administration at the NSLS. Beamline X16A is supported by AT&T Bell Laboratories. David Loretto is thanked for helpful discussion. C.S.D. wishes to acknowledge a grant from the Science and Engineering Research Council (UK). Research was carried out at the National Synchrotron Light Source, Brookhaven National Laboratory, which is supported by the US Department of Energy, Division of Material Sciences and Division of Chemical Sciences (DOE contract number DE-AC02-76CH00016). This work was also supported by the Director, Office of Basic Energy Sciences, Material Sciences Division of the US Department of Energy under contract No. AC03-76SF0098.

#### References

- [1] P.S. Peercy et al., *J. Mater. Res.* 5 (1990) 852.
- [2] J.L. Batstone, J.M. Phillips and E.C. Hunke, *Phys. Rev. Lett.* 60 (1988) 1394.
- [3] R.M. Tromp and M.C. Reuter, *Phys. Rev. Lett.* 61 (1988) 1756.
- [4] C.A. Lucas and D. Loretto, *Appl. Phys. Lett.* 60 (1992) 2071.
- [5] C.A. Lucas, G.C.L. Wong and D. Loretto, *Phys. Rev. Lett.*, in press.
- [6] M.H. Yang and C.P. Flynn, *Phys. Rev. Lett.* 62 (1989) 2476; *Phys. Rev. B* 41 (1990) 8500.
- [7] S. Fölsch, U. Barjenbruch and M. Henzler, *Thin Solid Films* 172 (1989) 123.
- [8] P.H. Fuoss and I.K. Robinson, *Nucl. Instrum. Methods* 222 (1984) 171.
- [9] R. Feidenhans'l, *Surf. Sci. Rep.* 10 (1989) 105.
- [10] I.K. Robinson, in: *Handbook on Synchrotron Radiation*, Vol. 3, Eds. D.E. Moncton and G.S. Brown (Elsevier, Amsterdam, 1991).
- [11] R.E. Schlier and H.E. Farnsworth, *J. Chem. Phys.* 30 (1959) 4.
- [12] F. Grey, R.L. Johnson, J. Skov Pedersen, R. Feidenhans'l and M. Nielsen, in: *The Structure of Surfaces II*, Eds. J.F. van der Veen and M.A. Van Hove (Springer, Berlin, 1988) p. 292.
- [13] S.D. Kevan, *Phys. Rev. B* 32 (1985) 2344.
- [14] W.R. Lambert, P.L. Trevor, M.J. Cardillo, A. Sakai and D.R. Hamann, *Phys. Rev. B* 35 (1987) 8055.

- [15] C.A. Lucas, C.S. Dower, D.F. McMorrow, G.C.L. Wong, F.J. Lamelas and P.H. Fuoss, *Phys. Rev. B*, in press.
- [16] I.P. Batra, *Phys. Rev. B* 39 (1989) 3919.
- [17] E.G. Michel, P. Pervan, G.R. Castro, R. Miranda and K. Wandelt, *Phys. Rev. B* 45 (1992) 11811.
- [18] R.D. Schnell, F.J. Himpsel, A. Bogen, D. Rieger and W. Steinmann, *Phys. Rev. B* 32 (1985) 8052.
- [19] For examples, see: *J. Phys. (Paris)* C7 (1989).
- [20] E. Vlieg, A.W. Denier van der Gon, J.F. van der Veen, J.E. Macdonald and C. Norris, *Phys. Rev. Lett.* 61 (1988) 2241.
- [21] I.M. Tidswell, B.M. Ocko, P.S. Pershan, S.R. Wasserman, G.M. Whitesides and J.D. Axe, *Phys. Rev. B* 41 (1990) 1111.
- [22] Y.-W. Mo, D.E. Savage, B.S. Schwartztruber and M.G. Lagally, *Phys. Rev. Lett.* 65 (1990) 1020.
- [23] M. Copel, M.C. Reuter, E. Kaxiras and R.M. Tromp, *Phys. Rev. Lett.* 63 (1989) 632.
- [24] B.E. Warren, *X-Ray Diffraction* (Addison-Wesley, Reading, MA, 1969) p. 190.
- [25] R.E. Martinez, E. Fontes, J.A. Golovchenko and J.R. Patel, *Phys. Rev. Lett.* 69 (1992) 1061.